THE JOURNAL OF BIOLOGICAL CHEMISTRY VOL. 282, NO. 29, pp. 21437–21447, July 20, 2007

Role of Laminin Terminal Globular Domains in Basement Membrane Assembly*[S]

Received for publication, April 9, 2007, and in revised form, May 16, 2007 Published, JBC Papers in Press, May 21, 2007, DOI 10.1074/jbc.M702963200

Karen K. McKee, David Harrison, Stephanie Capizzi, and Peter D. Yurchenco[1]

From the Department of Pathology and Laboratory Medicine, Robert Wood Johnson Medical School, Piscataway, New Jersey 08854

Laminins contribute to basement membrane assembly through interactions of their N- and C-terminal globular domains. To further analyze this process, recombinant laminin-111 heterotrimers with deletions and point mutations were generated by recombinant expression and evaluated for their ability to self-assemble, interact with nidogen-1 and type IV collagen, and form extracellular matrices on cultured Schwann cells by immunofluorescence and electron microscopy. Wild-type laminin and laminin without LG domains polymerized in contrast to laminins with deleted α1-, β1-, or γ1-LN domains or with duplicated β1- or α1-LN domains. Laminins with a full complement of LN and LG domains accumulated on cell surfaces substantially above those lacking either LN or LG domains and formed a lamina densa. Accumulation of type IV collagen onto the cell surface was found to require laminin with separate contributions arising from the presence of laminin LN domains, nidogen-1, and the nidogen-binding site in laminin. Collectively, the data support the hypothesis that basement membrane assembly depends on laminin self-assembly through formation of α-, β-, and γ-LN domain complexes and LG-mediated cell surface anchorage. Furthermore, type IV collagen recruitment into the laminin extracellular matrices appears to be mediated through a nidogen bridge with a lesser contribution arising from a direct interaction with laminin.

The laminins (Lm)[2] are a major family of basement membrane glycoproteins each consisting of α-, β-, and γ-subunits joined together through a coiled-coil (1). The α1-, α2-, α3B-, and α5-laminins possesses globular LN domains at the N terminus of each of the three subunits. In contrast, α4-laminins possess only two short arms because of truncation of the α-subunit short arm. All laminins terminate in a group of LG domains distal to the coiled-coil. Previous studies have shown that laminin-111 (Lm-111, α1β1γ1-subunit composition) self-assembles into a polymer (2–6). This polymerization is entropy-driven, thermally reversible, cooperative with a critical concentration of 0.1 μM, and calcium-dependent. The three-dimensional ultrastructure of the polymer was seen as a dense array of interconnecting struts in freeze-dried Pt/C replicas (4). Analysis of interactions among laminin proteolytic fragments supported a model of self-assembly in which the essential repeating complex of polymerization consists of the three LN domains joined together with each domain derived from a different laminin molecule (3). A subsequent study of different members of the laminin family led to a hypothesis that those truncated laminins lacking one or more short arms would not polymerize. More recently, evaluation of binding interactions between recombinant N-terminal laminin protein fragments by plasmon resonance spectroscopy and chemical cross-linking identified not only the proposed binding between α1-β1-, α1-γ1-, and β1-γ1-LN-LEa pairs, but also self-binding between fragments containing the α1-LN domain (7). This type of homologous inter-domain binding was also reported for recombinant α2-, α5-, and β2-subunit fragments and was interpreted as evidence that there was less stringency of short arm LN domain interaction required for polymerization than previously thought.

Type IV collagens are the only other basement membrane components known to self-assemble into a polymer. The network-like structure of $\alpha1_2\alpha2$[IV] collagen, consisting of 7 S domain complexes, NC1 dimers, and lateral associations, is considered to be an important element of the architecture of nearly all basement membranes (8, 9). Nidogen-1, a glycoprotein similar in structure to nidogen-2, binds to the γ-subunit short arm of laminin through its G3 domain, to type IV collagen through G2 and G3, and to perlecan (10–12). It was proposed that nidogen acts as a bridge between laminin and type IV collagen and as an organizer of basement membrane structure (13).

Most basement membranes contain more than a single laminin heterotrimer along with type IV collagens, nidogens, perlecan, and agrin. An exception is found in the basement membranes of the developing nematode embryo which lack type IV collagen until later stages and in which the laminin polymer may form the only scaffolding (14). Insights into the significance of basement membrane components and their interactions in tissues were gained through loss-of-function studies arising from mutations in mice, zebrafish, and invertebrates (reviewed in Ref. 15). Targeted inactivation of the *LAMC1* and

* This work was supported by National Institutes of Health Grant R37-DK36425. The costs of publication of this article were defrayed in part by the payment of page charges. This article must therefore be hereby marked "*advertisement*" in accordance with 18 U.S.C. Section 1734 solely to indicate this fact.

[S] The on-line version of this article (available at http://www.jbc.org) contains supplemental Table 1.

[1] To whom correspondence should be addressed: Dept. of Pathology and Laboratory Medicine, Robert Wood Johnson Medical School, 675 Hoes Lane, Piscataway, NJ 08854. Tel.: 732-235-5166 /4674; Fax: 732-235-4825; E-mail: yurchenc@umdnj.edu.

[2] The abbreviations used are: Lm, laminin; rLm, recombinant laminin; Δ, deletion; Σ, domain substitution; SC, Schwann cell; EHS, Engelbreth-Holm-Swarm; WT, wild type; HA, hemagglutinin; ECM, extracellular matrix; DAPI, 4,6-diamidino-2-phenylindole; PBS, phosphate-buffered saline; BM, basement membrane.

LAMB1 genes coding for the common γ1- and β1-laminin subunits revealed that laminins are essential for the formation of several embryonic basement membranes (16–18). In contrast, inactivation of the mouse genes for type IV collagen, nidogens, and the nidogen-binding site in the laminin γ1-subunit, although lethal by mid-embryonic development to birth, did not prevent basement membrane assembly in most tissues but instead caused structural defects and instability of basement membranes in different tissues (19–21). Genetic evidence supporting a role of laminin polymerization was found in the phenotype of the dy2J mouse in which defective basement membranes were observed in skeletal muscle and peripheral nerve Schwann cell endoneurium (reviewed in Ref. 15). The underlying genetic defect of dy2J is a splice-donor mutation resulting in an in-frame deletion within the α2-LN domain that has been correlated with a failure of α2-laminin polymerization (22, 23). Studies on embryoid bodies, a model of early embryonic development, and cultured Schwann cells have further implicated laminin polymerization as acting in concert with anchorage as key contributors to basement membrane assembly (24, 25).

An understanding of the assembly mechanisms is of value not only because of the role played by basement membranes in embryonic development and the pathogenesis of several diseases, but also because manipulations of assembly to produce more stable basement membranes hold promise as a therapeutic approach to correcting basement membrane defects (26). In this study we have focused on the contributions of laminin domains to the assembly process. Lm-111 heterotrimers were generated by recombinant expression in human embryonic kidney 293 cells and evaluated for their ability to polymerize, interact with nidogen-1 and type IV collagen, and form a basement membrane on cultured Schwann cells. These cells, involved in laminin-dependent congenital muscular dystrophy, were chosen because it has been found that native laminin-111 assembles a basement membrane-type ECM on the cell surfaces in culture, that laminin attachment to the cells (anchorage) is substantially mediated by sulfatides, and that dystroglycan, although not required for assembly, associates with this ECM resulting in the functional readouts of Src activation and utrophin recruitment (25). β1 integrins were not found to contribute to basement membrane assembly in this model.

The data of this study support the hypothesis that all three LN domains are essential for laminin polymerization and formation of a basement membrane. They also reveal a requirement of the laminin LG domains for basement membrane assembly consistent with the concept that laminin becomes tethered to the cell surface through its LG domains, whereas type IV collagen and nidogen become tethered primarily to laminin. In addition, the data provide cellular evidence for the importance of nidogen serving as a bridge between the laminin and type IV collagen polymers.

EXPERIMENTAL PROCEDURES

DNA Constructs

The wild-type cDNAs for mouse laminin α1, human β1, and human γ1 (mα1-pCIS, hβ1-pCIS, hβ1-pCEP4, hγ1-pRc/CMV2, γ1-wt$_{Cf}$, and α1-wt$_{Nf}$) have been described previously (27–29). Refer to supplemental Table 1 for details of laminin constructs. Restriction enzymes, T4 DNA ligase, and calf intestinal alkaline phosphatase were obtained from New England Biolabs and Fermentas. PCRs were carried out using PlatPfx (Invitrogen) and a PTC-100 thermal cycler (MJ Research).

α1-wt$_{Nm}$—The 5′-end of the mα1 cDNA was amplified from mα1-pCIS utilizing primers ma1p4 and ma1F21. Three subsequent overlapping PCRs with primers ha1p8, ha1p9, and ha1p6 were carried out to synthesize a 5′-fragment that contained a NotI site followed by a 5′-untranslated region, BM40 signal sequence, c-Myc epitope tag, enterokinase cleavage site, and the 5′-terminal region of mα1. The 3′-end of the mα1 was amplified with primers ma1F20 and ma1F25. Both PCR fragments were digested with NotI and BspHI. A BspHI restriction fragment from mα1-pCIS was gel-purified (UltraClean 15 DNA purification kit, MO BIO Laboratories, Inc.) and ligated into a NotI-digested DHpuro vector (described below) along with the 5′ and 3′ PCR products. The ligated material was transformed into DH5α bacteria (Invitrogen) and plated onto LB-agar plates containing 10 μg/ml ampicillin (Sigma), and resistant clones were isolated and grown in LB media, and DNA minipreps were performed with an UltraClean miniplasmid prep kit (MO BIO Laboratories, Inc.). Ligation junctions and PCR products were checked by restriction digestion and DNA sequencing.

α1ΔLN$_{Nm}$—NheI and BstEII-NheI fragment were isolated from α1-wt$_{Nm}$. Primers ma1F90 and 050604-13 were used in a PCR of mα1-pCIS to generate a fragment which was subsequently amplified with overlapping primer ma1F35 and then 050604-11 along with 050604-13 to generate the required 5′ sequence. The final PCR product was digested with NheI and BstEII and ligated with the other two isolated RE fragments.

α1ΔLN-L4b$_{Nm}$—A PCR fragment was produced from α1-wt$_{Nm}$ with primers da1-1f and da1–2r and sewn together with a second fragment, generated with da1–2f and da1-1r, using da1-1f and da1-1r and digested with AflII. An AflII fragment was isolated from α1-wt$_{Nm}$. Both fragments were ligated into an AflII prepared α1-wt$_{Nm}$.

α1ΔLG1-5$_{Nf}$—An AflII-SacII fragment of mα1-pRCX3 (27) was replaced with a PCR fragment generated from the same construct but utilizing a PCR primer to introduce a new SacII site and a STOP codon after the end of the coiled-coil domain.

α1ΔLG1-5$_{Nm}$—An AflII-AgeI fragment from α1-wt$_{Nm}$ was replaced with a PCR insert produced by ligating two PCR fragments. One fragment was generated with dg1 and dg2 and a second with dg3 and dg4, and both fragments were combined with dg1 and dg4.

β1-wt$_{Nh}$—An N-terminal PCR fragment containing a hemagglutinin epitope tag (HA; Roche Applied Science) was generated from hβ1-pCIS using four successive rounds of PCR with four sense primers (hb1-1, hb1-2, hb1-3, and hb1-4) and a single antisense primer (hb1-re1) and digested with NheI and EcoRI. A 3′-end PCR fragment was generated with hb1-re4 and hb1-10 and digested with MluI and KpnI. An EcoRI-MluI fragment was purified from hβ1-pCIS and ligated along with the two PCR fragments into the expression vector pcDNA3.1/zeo+ (Invitrogen), which had earlier been digested with NheI and KpnI.

β1ΔLN$_{Nh}$—The same approach used to generate β1-wt$_{Nh}$ was employed, except hb1-23, hb1-25, hb1-3, hb1-4, and hb1-re5 were used to generate the N-terminal PCR fragment that was digested with NheI and AatII. Also, an AatII-MluI fragment isolated from hβ1-pCIS was used. Both the C-terminal PCR fragment and prepared vector, used in constructing β1-wt$_{Nh}$, were utilized.

β1ΔLN-LEa$_{Nh}$—The same approach used to generate β1-wt$_{Nh}$ was employed, except hb1-28, hb1-30, hb1-3, hb1-4, and hb1-re7 were utilized to generate the N-terminal segment that was digested with NheI and BstEII. Likewise, a BstEII-MluI fragment was isolated from hβ1-pCIS.

γ1-ΔLN$_{Cf}$—A NotI restriction digest fragment was isolated from γ1-wt$_{Cf}$ as well as an ApaLI-NotI fragment. An N-terminal fragment was generated by two overlapping PCRs with gg1, gg3, and gg6 followed by digestion with NotI and ApaLI and ligation with the two isolated restriction fragments.

γ1-ΔLN-LEa$_{Cf}$—A NotI restriction digest fragment was isolated from γ1-wt$_{Cf}$ as well as an AflII-NotI fragment. A 5′-terminal fragment was generated by two overlapping PCRs with gg9, gg4, and gg5 followed by digestion with NotI and AflII and ligation with the two isolated restriction fragments.

γ1Σa1LN$_{Cf}$—A PCR fragment was produced from mα1-pCIS with primers a1s-1F and a1s-2R. A second fragment was generated from γ1-wt$_{Cf}$ with a1s-2F and a1s-1R. The two fragments were sewn together with primers als-1F and a1s-1R. The PCR fragment and γ1-wt$_{Cf}$ were both digested with SacII and AflII. The PCR fragment was then used to replace the corresponding fragment in γ1-wt$_{Cf}$.

γ1Σβ1LN$_{Cf}$—A PCR fragment was produced from hβ1-pCIS with primers b1s-1F and b1s-2R. A second fragment was generated from γ1-wt$_{Cf}$ with b1s-2F and b1s-1R. The two fragments were ligated with primers bls-1F and b1s-1R. The PCR fragment and γ1-wt$_{Cf}$ were both digested with SacII and BsrGI. The PCR fragment was used to replace the corresponding fragment in γ1-wt$_{Cf}$.

γ1-N802S$_{Cf}$ and γ1-P801Q$_{Cf}$—To generate N802S (Asn to Ser; AAC to AGC) or P801Q (Pro to Gln; CCC to CAG), a BsiMI-AflII PCR fragment derived from ligating two overlapping PCR-generated fragments was utilized to replace the corresponding BsiMI-AflII fragment in γ1-wt$_{Cf}$. The 5′-fragment was generated with Nd-1f and PQ-2r or NS-2r. Likewise, the 3′-fragment was generated with PQ-2f or NS-2f and Nd-1r. Both 5′- and 3′-fragments were combined with Nd-1f and Nd-1r and digested with BsiMI and AflII.

DHpuro—A vector that imparts puromycin resistance was constructed by replacing an AvrI-PciI fragment of pcDNA3.1/Hygro (Invitrogen) with a PCR fragment synthesized from pPUR (Clontech) containing the removed SV40 promoter sequence, puromycin resistance gene, an SV40 polyadenylation signal sequence, and a PciI site.

Recombinant and Native Proteins

Human embryonic kidney cells (HEK293) were cultured in Dulbecco's modified Eagle's medium (Invitrogen) supplemented with 10% fetal bovine serum (Atlanta Biological), 200 mM L-glutamine, and penicillin-streptomycin (1,000 units/ml penicillin and 1,000 μg/ml streptomycin; Invitrogen). (*a*) Plasmids containing laminin subunits were stably transfected into HEK293 cells with Lipofectamine 2000 (Invitrogen) according to the manufacturer's instructions. Stable cell lines expressing recombinant laminins were supplemented with puromycin (α1 chains), Zeocin (β1 chains), and G418 (γ1 chains) at a final concentration of 1, 100, and 500 μg/ml, respectively. Immunoprecipitation, SDS-PAGE, and Western blot analysis of secreted protein was used to confirm expression of trimeric laminin in the stable cell lines. The α1-, β1-, and γ1-laminin chains were detected with antibodies specific for Myc (Roche Applied Science), HA (Roche Applied Science), and FLAG (Sigma) epitopes, respectively. Recombinant laminin was purified from media on a heparin-agarose (Sigma) column and eluted with 500 mM NaCl (in 50 mM Tris, pH 7.4, 1 mM EDTA). Heparin-eluted rLm1 was further bound to FLAG M2-agarose (Invitrogen) and eluted with 100 μg/ml FLAG peptide in wash buffer (150 mM NaCl, 50 mM Tris, pH 7.4, 1 mM EDTA). The diluted protein was concentrated in an Amicon Ultra-15 filter (100,000, molecular weight cut-off) and dialyzed in TBS50 (90 mM NaCl, 50 mM Tris, pH 7.4, 0.125 mM EDTA). (*b*) A pCIS vector encoding full-length mouse nidogen-1 (gift of Rupert Timpl, Max Planck Institute for Biochemistry, Martinsried, Germany) was used to stably transfect cells. Secreted protein was purified from medium by metal chelating chromatography as described (10). (*c*) Type IV collagen was extracted from lathyritic mouse EHS tumor and purified by salt fractionation and DEAE-cellulose chromatography as described (30). (*d*) Laminin-111 was extracted with EDTA from lathyritic EHS tumor and purified by gel filtration and DEAE-Sephacel chromatography (unbound fraction) as described (3).

Protein Assays

Laminin, type IV collagen, and nidogen-1 concentrations were determined by absorbance at 280 nm, amino acid analysis, and comparison against known standards in Coomassie Blue-stained gels as described (2, 3, 30). Proteins were solubilized in Laemmli sample buffer and evaluated by SDS-PAGE under reducing conditions on 6% acrylamide gels. Electrophoresed gels were stained with Coomassie Brilliant Blue R-250, imaged with Bio-Rad Gel Doc 2000 in bright field mode, and analyzed with Quantity One software (Bio-Rad).

Laminin Polymerization, Type IV Collagen-Laminin, and Nidogen-binding Assays

Aliquots (50 μl) of laminin in polymerization buffer (TBS, 1 mM $CaCl_2$, 0.1% Triton X-100) at various concentrations were incubated at 37 °C in 0.5-ml Eppendorf tubes. Samples were centrifuged at 11,000 × *g* followed by dissolution of supernatant and pelleted fractions in SDS and analysis by SDS-PAGE. Similarly, increasing quantities of type IV collagen with constant laminin and nidogen (0.1 and 0.02 mg/ml, respectively) were incubated in PBS (with 0.1% Triton X-100) and analyzed as above. The Coomassie Blue-stained laminin β1 band and collagen α2 bands, which migrate separately, were used to determine the laminin and collagen amounts in the supernatant and pellet fractions. Nidogen binding to laminin was determined by immunoblotting. One μg of recombinant laminin was slot-blotted onto a polyvinylidene difluoride membrane (Bio-

Rad). Following a 1-h blocking step with 5% milk in TTBS (50 mM Tris, pH 7.4, 90 mM NaCl, 0.05% Tween 20), the laminin slots were incubated with various quantities of nidogen. Bound nidogen was detected with rabbit polyclonal antibody at 5 μg/ml and anti-rabbit horseradish peroxidase (Pierce) and quantitated by chemical luminescence in dark field mode with the Gel-Doc apparatus.

Cell Culturing

Schwann cells isolated from sciatic nerves from newborn Sprague-Dawley rats were the kind gift of Dr. James Salzer (New York University). These cells were expanded in culture for 10 passages and maintained in Dulbecco's modified Eagle's medium, 10% fetal calf serum (Gemini Bio Products), neuroregulin (0.5 μg/ml, Sigma), forskolin (0.2 μg/ml, Sigma), 1% glutamine, and penicillin-streptomycin. Cells at passages 11–17 were treated with laminin, type IV collagen, and/or nidogen-1 after plating onto 24-well dishes (Costar) at half-confluent density. The following day, the media were changed, and the cells were incubated with laminins (20–40 μg/ml), type IV collagen (10–20 μg/ml), and/or nidogen-1 (2–8 μg/ml) at 37 °C for 1 h followed by washing and fixation. For electron microscopy, SCs cells were plated in 60-mm Permanox dishes (Nalgene, Nunc) 2 days prior to addition of ECM proteins.

Antibodies and Immunofluorescence Microscopy

Schwann cells grown in the presence of extracellular proteins were rinsed three times with PBS (10 mM sodium phosphate, pH 7.4, 127 mM NaCl) and fixed in 3% paraformaldehyde for 30 min. Cultures were blocked with 5% goat serum and then stained with primary and appropriate secondary antibodies conjugated with fluorescent probes. Rabbit polyclonal antibodies specific for laminin-111 (EHS), laminin fragment E4 (β1LN-LEa), recombinant laminin α1LG4–5 (RG50), and nidogen-1 were used as described (24). EHS laminin antibody was titered in wells coated (1 μg/ml) with recombinant laminins (WTa, β1ΔLN, α1ΔLN, α1ΔLN-L4b, γ1ΔLN, and α1ΔLG1-5) and evaluated by direct enzyme-linked immunosorbent assay with serial 2-fold dilutions of antibody. The binding plots were essentially identical for all substrates except for α1ΔLN-L4b whose plot lagged by a single 2-fold dilution and whose color intensity at saturation (5 μg/ml) was decreased by <10%. This antibody (20 μg/ml) was used to compare the accumulation of different laminins on cell surfaces. Nidogen-specific rabbit antibody prepared against recombinant nidogen-1 (25) was used at 3 μg/ml, and type IV collagen-specific rabbit antibody (Chemicon) was used at a 1:100 dilution. Detection was accomplished with Alexa Fluor 488 and 647 goat anti-rabbit IgG secondary antibodies (Molecular Probes) at 1:500 and 1:100 respectively, and fluorescein isothiocyanate-conjugated donkey anti-mouse IgM at 1:100 (Jackson ImmunoResearch). Slides were counterstained with DAPI and imaged as described (24). Laminin, type IV collagen, and nidogen immunofluorescence levels were quantitated from digital images (average of 9, each 1300 × 1030 pixels, 437 × 346 μm) recorded using a ×20 microscope objective with IPLab 3.7 software (Scanalytics). A segmentation range was chosen to subtract background and acellular immunofluorescence. The sum of pixels and their intensities in highlighted cellular areas of fluorescence were measured and normalized by dividing by the number of cells determined by a count of DAPI-stained nuclei for each image. Data were expressed as the mean ± S.D. of normalized summed intensities with the data analyzed by one-way analysis of variance with Holm-Sidak comparisons in SigmaPlot version 9.01 and SigmaStat version 3.1 (Systat).

Electron Microscopy

For Rotary shadow Pt/C replicas, laminin (25–50 μg/ml in 0.15 M ammonium bicarbonate, 60% glycerol) was sprayed onto mica disks, evacuated in a BAF500K unit (Balzers), rotary-shadowed with 0.9 nm Pt/C at an 8° angle, and backed with 8 nm carbon at a 90° angle as otherwise described (3). Cells adherent to plastic were fixed in 0.5% glutaraldehyde and 0.2% tannic acid, transferred to modified Karnovsky's fixative, washed with PBS, post-fixed in 1% osmium tetroxide, and prepared for electron microscopy as described (31).

RESULTS

Protein sequences of the α1-, β1-, and γ1-subunits of laminin were modified as shown in Fig. 1. The new domain nomenclature described by Aumailley *et al.* (1) was used throughout the paper. Epitope tags were placed either at the N or C terminus of the subunits to aid in selection of 293 cell clones expressing one, two, or three subunits, with the FLAG tag used for purification of protein. Stable clones expressing laminin heterotrimers consisting of α1-, β1-, and γ1-subunits were selected and expanded (Fig. 1). Wild-type laminins containing either an N-terminal FLAG tag and no γ1 tag (WTa), or containing an N-terminal Myc tag with a γ1 C-terminal FLAG tag (WTb), or with an N-terminal FLAG tag with a γ1 C-terminal FLAG tag (WTc) were prepared. No differences in stability, polymerization, or ability to assemble BMs on Schwann cells (SCs) were appreciated. WTb laminin was used for subsequent studies unless otherwise indicated. Protein yields for the recombinant laminins were found to vary from 10 to 20 μg/ml in conditioned medium.

Characterization of Laminins—Recombinant heterotrimeric laminins were analyzed by SDS-PAGE (Fig. 2). The three subunits were detected with epitope-specific and laminin subunit-specific antibodies in which the laminin was immunoprecipitated with a subunit tag-specific antibody and the other chains detected in immunoblots (data not shown). Wild-type protein exhibited a typical Coomassie Blue-stained pattern of three bands corresponding to the α1-, β1-, and γ1-subunits. Deletion of different subunits resulted in the expected increased migration. Deletion of the β1-LN domain resulted in a superimposition of the normally faster migrating γ1 band by the shortened β1 band, and deletion of almost the entire α1 short arm (domains LN -L4b) resulted in superimposition of the α1 band on the β1 band. Laminins bearing γ1P801Q or N802S contained free α1 short arm fragments similar to those described previously (27). Rotary-shadowed Pt/C replicas were prepared and examined (Fig. 3) (data not shown) for WTa, WTb, β1ΔLN, β1ΔLN-LEa, γ1ΔLN-LEa, γ1ΔLN, α1ΔLN-L4b, α1ΔLN, γ1Σβ1LN, α1ΔLG1-5, γ1P801Q, and γ1N802S. All revealed a population of heterotrimers. Loss of the expected LN domains,

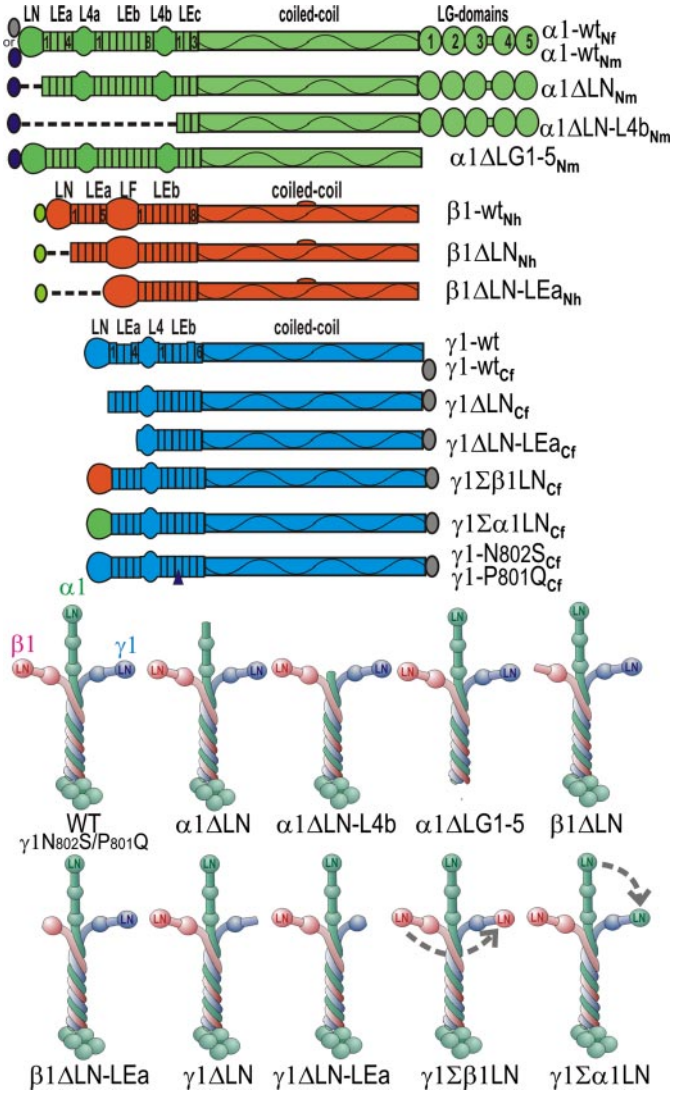

FIGURE 1. **Recombinant laminin subunits and heterotrimers.** Deletions (Δ), domain substitutions (Σ), and point mutations are indicated for the α1 (*green*), β1 (*red*), and γ1 (*blue*) subunits of laminin-111 with the derived heterotrimers shown below. The signal sequence of BM-40 was placed directly upstream of mature laminin sequences or epitope tags (FLAG (*f, gray*), HA (*h, green*), or Myc (*m, purple*) that formed the mature N-terminal sequence of laminin subunits. The 8-amino acid-long FLAG tag served as the best ligand for purification by affinity chromatography. Wild-type (*WT*) and β1ΔLN-LEa laminins were expressed with either an N-terminal FLAG tag combined with the no tag on the γ1-subunit (WTa) or, as used with the other laminins, an N-terminal Myc tag and a γ1 FLAG tag at the C terminus (WTb).

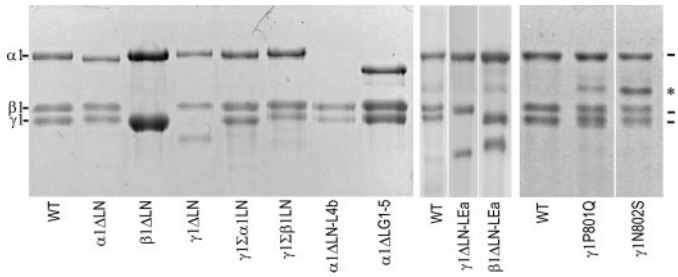

FIGURE 2. **SDS-PAGE of recombinant laminins.** Recombinant heterotrimeric laminins were subjected to electrophoresis on SDS-polyacrylamide gels under reducing conditions and stained with Coomassie Blue. Migration positions of wild-type (*WT*) α1-, β1-, and γ1-subunits are indicated on the *left* with identity of the modified subunits below. *Asterisk* indicates position of a free N-terminal fragment of the α-subunit seen in preparations of laminins with mutations of γ1LEb3.

LG domains, or α1-short arm could be detected in many of the well spread laminins and were most consistently obvious for α1ΔLG1-5 (Fig. 3, *arrows*).

Polymerization of Laminins—A standard assay of laminin polymerization was used to evaluate the recombinant laminins (Fig. 4) in which aliquots of laminin in the presence of calcium were incubated at 37 °C followed by separation of the polymer pellet from free laminin (supernatant) and quantitation of stained gels by densitometry (2). WT recombinant laminin polymerized in a concentration-dependent fashion (Fig. 4, *A–C* and *E–I*) with a slope of 0.81 ± 0.21 and an *x* axis intercept of 0.09 ± 0.03 mg/ml (average ± S.D., $n = 7$). This compared with 0.08 mg/ml ± 0.03 mg/ml ($n = 3$) for EHS laminin, similar to the critical concentration previously reported for EHS-derived laminin-111 (3, 4). Polymerization was prevented by incubating the recombinant laminin with 1 mM EDTA, confirming the divalent cation dependence of the reaction. Laminins with either a deletion of the LG domains (α1ΔLG) or bearing point mutations in γ1-LE3b (N802S and P801Q) also polymerized in a manner similar to WT laminin (Fig. 4, *D* and *F*) (data not shown). However, laminin α1ΔLN showed very little aggregation at the highest concentration analyzed (Fig. 4*I*), and the other laminins with single LN deletions (β1-LN, β1-LN-LEa, γ1-LN, and γ1-LN-LEa) did not polymerize in the concentration range analyzed (Fig. 4, *B*, *E*, and *G–I*). In addition, a laminin lacking almost the entire α-subunit short arm (α1ΔLN-L4b), a short arm model for the truncated α4-laminins found in a variety of tissues, did not polymerize (Fig. 4*B*). The effect of substituting the γ1-subunit LN by either β1-LN or α1-LN was evaluated. If the laminin polymer is a consequence of formation of a ternary complex of the three different LN domains, with one bond required between each LN pair, then either modification should result in a loss of polymerization. On the other hand, if the polymer employs the α1LN-α1LN interaction reported by Odenthal *et al.* (7), then replacement of the γ1-LN by the α1-LN (γ1Σα1LN) should not prevent polymerization. It was found that substitution of γ1-LN by α1-LN, similar to substitution of γ1LN by β1LN, resulted in a failure of polymerization (Fig. 4, *G* and *H*).

Nidogen Binding and Type IV Collagen Interactions—It has been shown previously that nidogen-1 binds to both laminins and to type IV collagen and that substitution of asparagine for serine (N802S) in the laminin γ1-LEb3 domain results in loss of binding to the protein nidogen-1 to laminin fragment P1, whereas substitution of the immediate adjacent amino acid proline for glutamine (P801Q) has no effect on nidogen binding (32). These two single amino acid substitutions were introduced into recombinant laminin-111 to determine whether this interaction might contribute to laminin polymerization and what effect the mutation might have on BM assembly. The recombinant nidogen-1 used to evaluate binding migrated with the expected molecular mass of 150 kDa with much lower levels of the ~80-kDa fragment (Fig. 5*A*). Binding of recombinant nidogen-1 to WT laminin, γ1P801Q, and γ1N802S was evaluated in a solid phase binding assay (Fig. 5*B*). The binding plots for WT and γ1P801Q laminins were similar (apparent dissociation constants of 6.5 and 2.9 nM,

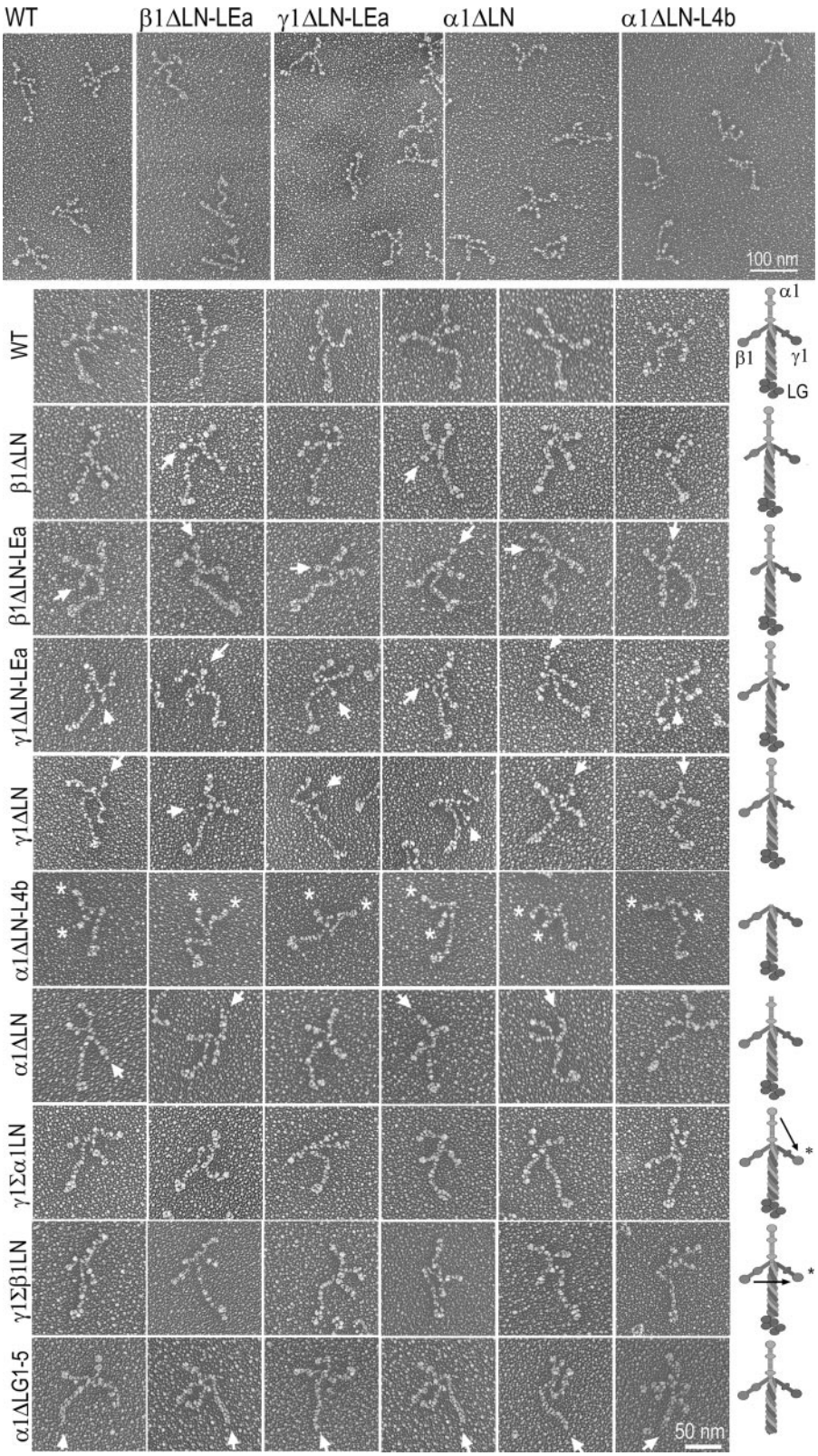

FIGURE 3. **Rotary shadow electron microscopy of laminin molecules.** Recombinant laminins were rotary-shadowed with Pt/C and examined by electron microscopy. Images of groups of recombinant laminins are shown in the *upper panels*. A gallery of images for individual recombinant laminin molecules is shown below. *Arrows* indicate missing domains where recognized, and *asterisks* indicate intact short arms in the α-short arm deletion mutant.

respectively), whereas the binding plot for γ1N802S revealed little or no interaction.

Type IV Collagen Interactions—Purified type IV collagen ($\alpha1_2\alpha2$[IV]) polymerized when incubated in PBS at 37 °C (Fig. 6, *A* and *B*) (30). When mixed with nidogen-1, a fraction of the nidogen was found in the polymer pellet. A modification of the assay to include WT or NS laminins in the presence or absence of nidogen-1 was used to detect the ability of the collagen polymer to form a complex with laminin through a nidogen bridge (Fig. 6*C*). The laminin was incubated at a concentration of 0.1 mg/ml, a concentration at which it normally does not polymerize. The highest fractions of WT laminin were detected in the collagen polymer pellet in the presence of nidogen-1 in contrast to low and similar fractions with incubations of NS laminin with nidogen, NS laminin without nidogen, or WT laminin without nidogen. It was concluded that nidogen mediated a laminin association with type IV collagen.

Laminin Accumulation on the Surface of Cultured Schwann Cells—It was found previously that incubation of SCs with exogenous laminin-111 results in the formation of a basement membrane-like ECM on the exposed free cell surface (25, 31). Interactions of laminins-1 and -2 with galactosyl sulfatide, a glycolipid found in the plasma membranes and known to bind to the LG-4 domain of laminin-1, was found to be a requirement for BM assembly on SCs (25). Cultured SCs were found to express no detectable endogenous laminin. Endogenous nidogen-1 and type IV collagen were only detected with overnight cell accumulations into media but not in the 1-h accumulations as used in this study (25).[3] To analyze the ability of modified laminins to assemble a BM, SCs were incubated with 20 μg/ml of different recombinant proteins (Fig. 7). Treatment of cells with WTa or WTb laminin resulted in nearly

[3] K. K. McKee, D. Harrison, S. Capizzi, and P. D. Yurchenco, unpublished observations.

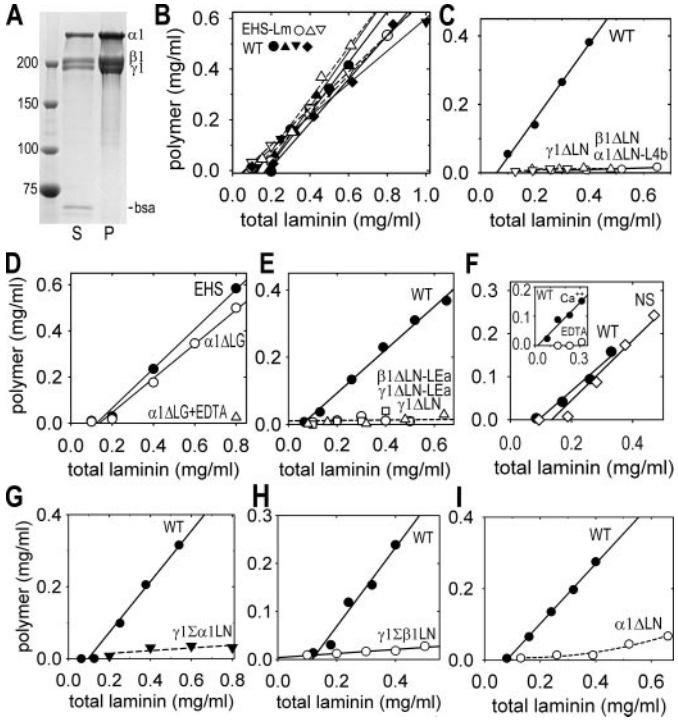

FIGURE 4. **Laminin polymerization.** Recombinant laminins and EHS laminin were incubated in the presence of 1 mM calcium (or 5 mM EDTA where indicated) at 37 °C followed by centrifugation, SDS-PAGE, and quantitation of Coomassie Blue intensity of supernatant (*S*) and pellet (*P*) fractions. *A*, Coomassie Blue-stained gel of WT laminin following incubation. Plots of concentration of polymer as a function of total laminin concentration (*B–I*) are shown for the indicated laminins. *B* compares different EHS laminin and WT laminin preparations. EHS laminin, wild-type (*WT*) recombinant laminin, laminin lacking LG1-5 (α1ΔLG), and laminin unable to bind to nidogen (γ1N802S, *NS*) polymerized, whereas laminins bearing deletions of any LN domain (α1ΔLN, α1ΔLN-L4b, β1ΔLN, β1ΔLN-LEa, γ1ΔLN, and γ1ΔLN-LEa) or substitution of an LN domain (γ1Σα1LN and γ1Σβ1LN) did not polymerize.

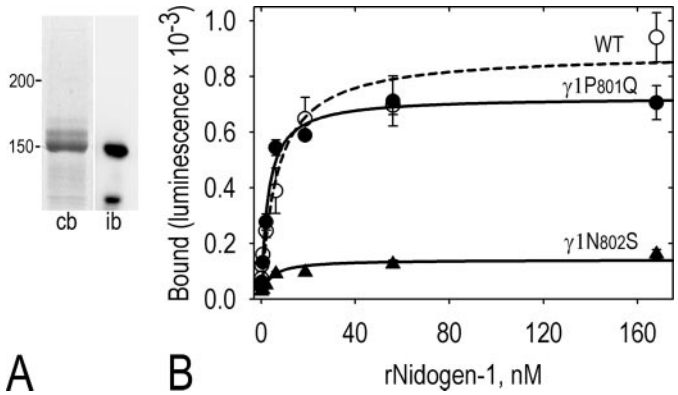

FIGURE 5. **Nidogen-binding of laminins bearing point mutations in γ1-domain LEb.** *A*, comparison of a Coomassie Blue (*cb*)-stained gel (SDS-PAGE, reducing) of recombinant nidogen-1 with an immunoblot (*ib*). *B*, recombinant WT laminin (rLm1/wt) or laminin bearing point mutations within γ1LEb3 (γ1P801Q and γ1N802S) were dot-blotted onto polyvinyl difluoride membranes and incubated with the indicated concentrations of recombinant nidogen-1 followed by antibody detection. Simple ligand binding fits of the relative luminescence intensity plotted against nidogen concentration are shown (average ± S.D., $n = 3$).

identical levels of fluorescence (data not shown). WTb laminin fluorescence was then compared with that produced by incubation with equal concentrations of laminins with the mutations α1ΔLN, β1ΔLN, γ1ΔLN, α1ΔLN-L4b, γ1Σα1LN, γ1Σβ1LN, and α1ΔLG1-5. High immunofluorescence was

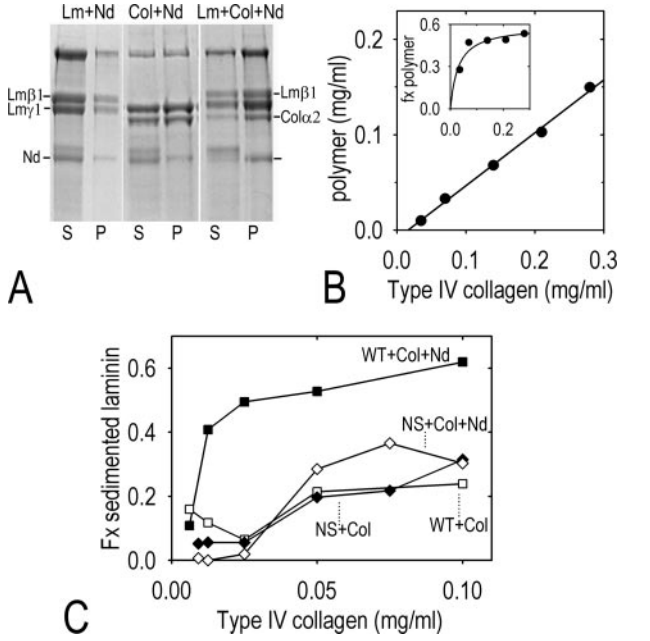

FIGURE 6. **Type IV collagen interactions.** *A*, aliquots of WT laminin (0.2 mg/ml) incubated with nidogen (0.04 mg/ml), type IV collagen (0.18 mg/ml) incubated with nidogen-1 (0.04 mg/ml), and laminin (0.16 mg/ml), nidogen (0.03 mg/ml), and collagen (0.16 mg/ml) were centrifuged to separate supernatant (*S*) from polymer (*P*) fractions and analyzed by SDS-PAGE under reducing conditions. Coomassie Blue-stained lanes are shown. *B*, aliquots of type IV collagen, incubated at 37 °C for 1 h, were analyzed as above with polymer (*P*, pellet) plotted against total protein (fraction polymer, *Fx*, shown in *inset*). *C*, type IV collagen was incubated at increasing concentrations in the presence or absence of nidogen (0.02 mg/ml) and/or WT or NS laminin (0.1 mg/ml), centrifuged, and analyzed as above. Plots of the fraction of laminin within the collagen polymer pellet are shown. Higher fractions of laminin associated with the collagen pellet if nidogen and the nidogen-binding site in laminin were present.

observed with WT laminin and not with the other conditions evaluated ($p < 0.001$).

The contributions of nidogen-1 and type IV collagen to basement membrane component accumulation of SC surfaces were also examined (Fig. 8). Representative immuno-stained cells are shown for some of the conditions (Fig. 8*A*) shown in Fig. 8, *B–D*. The highest laminin immunofluorescence resulted from treatment of cells with a mixture of WT laminin with or without nidogen-1 and type IV collagen (Fig. 8*B*). Although a small increase of laminin immunofluorescence appeared to be present in several experimental sets because of co-incubation with nidogen and collagen (compared with laminin treatment alone), the differences were not found to be significant within data sets (Fig. 8*B*) (data not shown). Addition of nidogen-1 to the laminin resulted in a small decrease in laminin immunofluorescence. The highest nidogen immunofluorescence level (Fig. 8*C*) was observed when nidogen was incubated with laminin and collagen ($p < 0.001$, compared with other conditions). Nidogen immunofluorescence was reduced to an intermediate level if only laminin and nidogen were present (32 ± 6% compared with WT laminin + nidogen + collagen, $p < 0.001$), and essentially absent (0.2 ± 0.1%, $p < 0.001$) if N802S laminin was incubated in place of WT laminin with nidogen and type IV collagen. Type IV collagen levels were highest (Fig. 8*D*) when incubated with WT laminin and nidogen ($p < 0.001$, compared with other conditions). They were reduced if the collagen was

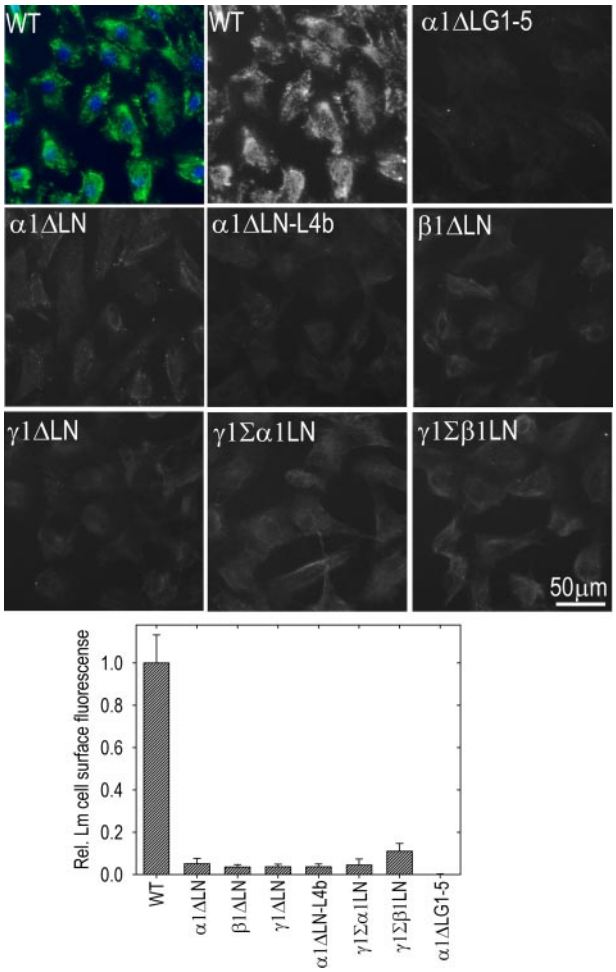

FIGURE 7. **Immunofluorescence detection of laminin assembly on Schwann cell surfaces.** SCs were incubated with the indicated recombinant laminins for 1 h and immunostained with laminin-specific antibody with a DAPI counterstain (example of co-staining shown in *upper left panel*). Quantitation of antibody fluorescence summed intensities divided by number of DAPI-stained nuclei (average ± S.D., $n \geq 7$ each condition) is shown below. Wild-type laminin treatment resulted in strong immunofluorescence compared with all other conditions.

incubated with laminin-γ1N802S and nidogen (33 ± 4% compared with WT laminin + nidogen + collagen, $p < 0.001$) or if incubated with WT laminin in the absence of nidogen (25 ± 11% compared with WT laminin + nidogen + collagen, $p < 0.001$). Collagen immunofluorescence was further reduced if the collagen was incubated with laminin α1ΔLG1-5 and nidogen (12 ± 4% compared with WT laminin + nidogen + collagen, $p < 0.001$), a level not significantly different from the base-line values observed with collagen + nidogen (7 ± 3%). Type IV collagen levels were also low when the collagen was incubated with nidogen and the nonpolymerizing laminin α1ΔLN, but higher than that observed when the collagen was incubated with nidogen and α1ΔLG1-5 (40 ± 9% *versus* 12 ± 4%, $p < 0.002$).

Taken together, the data are interpreted as evidence that substantial laminin accumulates on the cell surface in the absence of type IV collagen or nidogen but that collagen and nidogen accumulation on the cell surface requires laminin. The results reflect several requirements for nidogen recruitment onto the SC surface, *i.e.* laminin and the nidogen-binding site, an interaction further enhanced by the presence of type IV collagen. The data also reflect several contributions to type IV collagen recruitment onto the SC surface, *i.e.* laminin, laminin polymerization, nidogen, the nidogen-binding site in laminin, and the LG domains of laminin. However, collagen recruitment does not entirely depend upon nidogen because low levels were detected when a nidogen-binding mutant of laminin replaced WT laminin.

An unexpected finding was that a modest increase of collagen cell surface recruitment occurred when the protein was incubated with a nonpolymerizing laminin in the presence of nidogen. This was explored further (Fig. 8*E*) by varying the nidogen concentration in the presence of constant laminin γ1ΔLN (40 μg/ml) and type IV collagen (20 μg/ml). Under these conditions the laminin immunofluorescence remained nearly the same, whereas the type IV collagen level increased noticeably with nidogen concentrations that exceeded 1 μg/ml. A possible mechanism to explain this is that a low surface density of anchored laminin, unable to polymerize on its own, can bind to type IV collagen through nidogen, allowing formation of a limited amount of collagen-rich but laminin-poor ECM.

Ultrastructure—Cross-sections of cells treated with recombinant laminins were examined by electron microscopy (Fig. 9). Extracellular matrices appeared similar to those reported previously (24, 31) as continuous or near-continuous linear densities (lamina densa) separated by a thin lucent line (lamina lucida) from the edge of the adjacent plasma membrane. These were considered to represent "nascent" basement membranes. A lamina densa was observed following treatment with recombinant laminin WTa laminin, WTb laminin, γ1N802S laminin, and EHS-Lm-111 (Fig. 8) (data not shown). Short linear densities or, more commonly, only small aggregates were observed on cells treated with laminins α1ΔLN, β1ΔLN-LEa, and γ1ΔLN-LEa, and only scattered small discrete extracellular aggregates were present on exposed cell surfaces of cells treated with α1ΔLG1-5 laminin. Addition of type IV collagen and nidogen to WT laminin resulted in cells with long linear stretches of extracellular matrix (generally denser than that observed with laminin alone) adjacent to the plasma membrane, whereas addition of type IV collagen and nidogen alone resulted in cell surfaces with infrequent scattered extracellular aggregates. Addition of nonpolymerizing laminin α1ΔLN together with nidogen and type IV collagen resulted in appearance of longer, less electron-dense linear densities along the cell surface in a generally more discontinuous distribution. Treatment of cells with a mixture of laminin α1ΔLG1-5 with nidogen and type IV collagen resulted in the appearance of only scattered aggregates.

DISCUSSION

A correlation was made in this study between binding and self-assembling activities detected in basement membrane components by biochemical means with behavior of the components in a condition-limited cellular model of basement membrane assembly. The short arms of laminins, consisting of N-terminal globular LN domains and internal globular domains separated by LE rod-like repeats, were found to provide the activities of polymerization and nidogen binding,

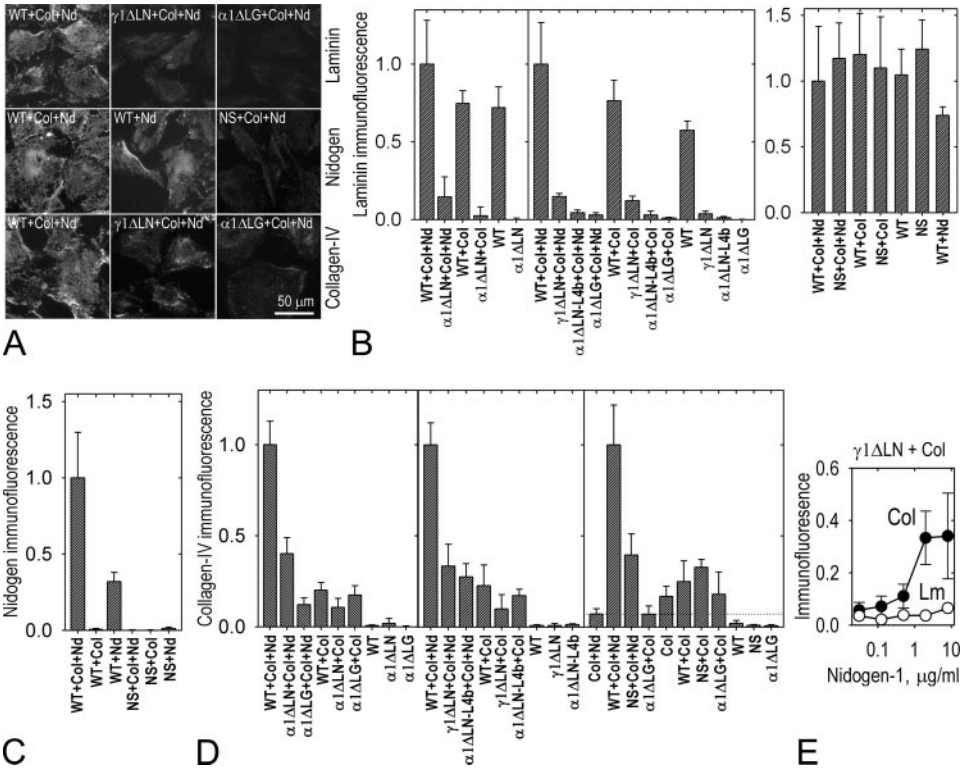

FIGURE 8. **Contributions of type IV collagen and nidogen-1 to ECM assembly.** SCs were incubated for 1 h with mixtures of laminins (20 μg/ml; *Lm*), nidogen-1 (2 μg/ml; *Nd*), and type IV collagen (10 μg/ml; *Col-IV*) as indicated. Representative images of cell immunofluorescence are shown in *A*. Quantitation of immunofluorescence (average and standard deviations of the sums of pixel intensities divided by number of DAPI-stained nuclei for cells treated with the indicated combinations of laminins, type IV collagen, and nidogen-1 shown in *B* (laminin immunostaining, $n \geq 5$ for each condition), *C* (nidogen immunostaining, $n \geq 5$), and *D*, (type IV collagen immunostaining, $n \geq 6$). High laminin immunofluorescence (*B*) was detected for all conditions in which the cells were incubated with WT or NS laminin. High nidogen immunofluorescence (*C*) was detected when nidogen was co-incubated with WT laminin and collagen, but not if nidogen was incubated with NS laminin and collagen. High collagen immunofluorescence (*D*) was detected when type IV collagen was incubated with WT laminin with nidogen, was reduced when incubated with WT laminin alone, and was nearly absent when the collagen was incubated with α1ΔLG1-5 and nidogen. Increasing the nidogen concentration (*E*) with fixed concentrations of γ1ΔLN laminin (40 μg/ml) and type IV collagen (20 μg/ml) resulted in a progressive but small increase in laminin immunofluorescence and a moderate increase in collagen immunofluorescence.

whereas the LG domains are known to provide binding sites for cell surface receptors and sulfatides. The results support a model (Fig. 10) in which the three LN domains mediate laminin polymerization, an activity of laminin that is required for the formation of a laminin scaffolding and that contributes to overall basement membrane assembly. The study also reveals that laminin binding to nidogen can promote efficient incorporation of type IV collagen into a laminin ECM with a lesser contribution arising from a laminin-collagen interaction.

Earlier studies to map laminin polymerization loci were hampered by a lack of suitable and well defined protein reagents, forcing reliance on analysis of protein fragments. To overcome this deficit and to allow evaluation of an assembly process that requires simultaneous contributions from three different subunits, the approach of generating a panel of recombinant heterotrimeric laminins was taken in which polymerization and nidogen interactions were evaluated *in vitro* and correlated with the ability of these laminins to mediate basement membranes on living cell surfaces. Several requirements for laminin polymerization were revealed by this approach. First, the LN domains, as previously suspected, are essential for laminin polymerization. Removal of any LN domain results in a failure of polymerization. Second, polymerization requires the combined contributions of the α1-, β1-, and γ1-LN domains. Replacement of the γ1-LN domain by a β1-LN or α1-LN domain results in a failure of polymerization even though the mutated laminin possesses three LN domains. An earlier investigation of laminin fragment complexes formed by incubating Lm-111 fragments E4 (containing β1-LN-LEa) and E1′ (α1 and γ1 short arm complex) identified a ternary complex with what appeared to be a favored association of the α1-, β1-, and γ1-LN domains (3). The current study reinforces the earlier conclusions using heterotrimeric reagents, and a model to explain the association is that one bond exists between each LN domain, *i.e.* α1-β1, α1-γ1, and β1-γ1, with each required to provide the cooperative affinities required for polymerization.

The observation here that the combination of two α1-LN domains and one β1-LN domain did not result in polymerization does not support an inference arising from the study of Odenthal *et al.* (7) that α-subunit self-association contributes to polymerization. It may be that not all binary binding interactions detected with the isolated fragments are essential for polymerization and that there may exist a further restriction of specificity arising from the geometry of polymerization in which only those binding sites with a correct azimuthal orientation interact to form a polymer or, alternatively, further specificity might arise from other short arm domain contributions. The additional finding that deletion of almost the entire α-subunit short arm in a laminin, whose domain structure is similar to several truncated laminins, is little different from deletion of the α-subunit LN domain further supports the conclusion based only on co-polymerization studies that laminins bearing only two short arms cannot polymerize (2). Thus, loss of polymerization, regardless of how it is achieved, results in a failure of nascent (collagen-free) basement membrane assembly on the free surface of cultured cells. A similar observation with these recombinant laminins was made following their incubation with cultured C2C12 myotubes.[3]

Nascent basement membrane assembly was also found to require the presence of the LG domains, *i.e.* polymerization is necessary but not sufficient. The LG domain complex, containing major cell-interactive loci, likely contributes to assembly by

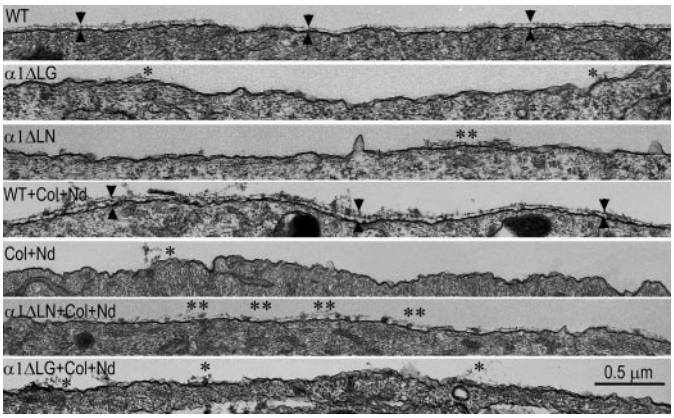

FIGURE 9. **Surface ultrastructure of laminin-treated cells.** SCs were treated with wild-type (*WT*) and modified laminins (40 μg/ml) alone or in the presence of type IV collagen (*Col,* 20 μg/ml) and/or nidogen-1 (*Nd*, 4 μg/ml) and incubated for 1 h. Representative images of the free cell surfaces are shown. A *thin continuous* electron-dense *line* (lamina densa, *upper arrowheads*) is seen adjacent to the plasma membrane (*lower arrowheads*) in cells following treatment with WT recombinant laminin-111. Scattered small extracellular aggregates (*) or short lengths of lamina densa (**) are present on cell surfaces treated with nonpolymerizing laminins or cells treated with α1ΔLG1-5 (α1ΔLG). A lamina densa is seen on cells treated with a mixture of WT laminin, type IV collagen, and nidogen-1, and a discontinuous lamina densa of low electron density following treatment with a nonpolymerizing laminin (*α1ΔLN*) with collagen and nidogen is also shown.

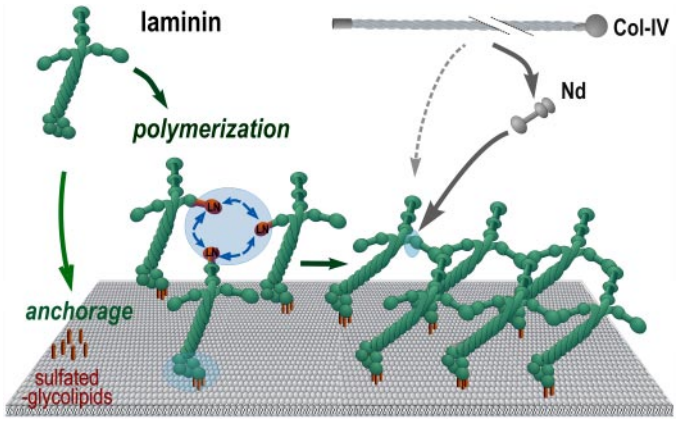

FIGURE 10. **Basement membrane assembly.** A model is shown based upon interactions evaluated *in vitro* and in a defined cultured cell system. Laminin molecules form an initial nascent ECM scaffolding through the binding of their LG domains to the cell surface (anchorage) and through polymerization in which each short arm forms an α-β-γ LN ternary domain complex with the short arms of two adjacent laminins. Type IV collagen (*Col-IV*) molecules associate with the laminin polymer primarily through the bridging activity of nidogens (*Nd*, *broad arrows*) but also through a direct interaction (*thin light arrows*) with the laminin network. This enables formation of a collagen copolymer, an important contributor to basement membrane stability. Potential contributions of perlecan and agrin, not investigated in this study, include further linkage of type IV collagen to laminin (*light gray arrows*) and stabilization of anchorage, respectively. Receptor-mediated contributions of integrins and dystroglycan are not included in the illustration.

serving to anchor the laminin to the cell surface (25). Recent studies of our laboratory group revealed that anchorage in SCs is substantially provided by sulfated glycolipids rather than by integrins, heparan sulfates, or dystroglycan (24, 25, 33). Several arginine- and lysine-rich loci recently mapped to the LG4 protein surface are responsible for sulfatide binding (33). When laminins are incubated with SCs, very little accumulation of laminin on the surface is detected in the absence of polymerization. This low level has been attributed to the cooperativity of binding resulting from polymerization and anchorage, first proposed based on observations made with laminin assembly on synthetic galactosyl sulfatide bilayers and providing an interpretation for the finding that inhibition of laminin polymerization or LG activities with fragments that block basement membrane formation (34). That study revealed that assembly on a laminin-binding lipid bilayer occurred as much as 10-fold below its solution critical concentration (providing a basis to explain how laminins can assemble a nascent basement membrane below their solution critical concentration as occurred in this study). Another possible mechanism, not exclusive of the first, is that cell surfaces possess only a limited number of laminin-binding sites relative to the number of laminins required to pack within a nascent basement membrane, *i.e.* most laminins are retained in the nascent scaffolding indirectly through LN domain-mediated associations and without LG anchorage. Loss of polymerization would therefore result in loss of all laminins except the small number that are anchored to the cell surface.

Type IV collagen, alone or mixed with nidogen-1, did not form an ECM on SC surfaces. This is consistent with observations made in mice that basement membranes are not formed in the absence of laminins (17, 18). However, a distinction needed to be made between the requirement for laminin *versus* laminin polymerization. In particular, it is conceivable that type IV collagen can separately drive assembly of an extracellular scaffold through its own polymerization if allowed to bind to a nonpolymerizing laminin that indirectly provides anchorage to the cell surface. In this study, ECM cell assembly was found to be substantially dependent on contributions arising from laminin polymerization, with reduced collagen and even lower laminin incorporation observed with nonpolymerizing laminins. Nonetheless, there was evidence for a limited degree of collagen compensation resulting in formation of an attenuated and discontinuous ECM. This ECM can be compared with the less severely attenuated basement membranes observed in skeletal muscles and peripheral nerve Schwann sheaths of the dy2J mouse that expresses α2-laminin bearing a truncation of the α2-subunit LN domain. However, in the latter the basement membrane also contains α4-laminins as well, and it may be that "compensatory" activity of type IV collagen is not sufficient to enable assembly of a functionally active and stable basement membrane in the absence of other contributions. A related issue concerns the mechanism by which nonpolymerizing laminins such as the α4-laminins might mediate basement membrane assembly. Although the laminin (α1ΔLN-L4b) evaluated to address this question was unable to polymerize or form a nascent basement membrane, and supported only a small increase in collagen recruitment to the cell surface, one needs to consider the possibility that nidogen-binding and hence collagen-recruiting truncated laminins possess either greater affinity for cell surfaces and/or interact with a larger repertoire of cell surface molecules compared with laminin-111, allowing bypass of the polymerization requirement for ECM assembly. Support for such a concept can be found in the rescue of the muscle basement membrane in the α2-laminin mutant mouse achieved by transgenic overexpression of the laminin and cell-binding mini-agrin (26).

A prominent role of nidogen in enabling type IV collagen recruitment to the basement membrane, as seen in this study, was previously predicted based on the binding repertoire of nidogen (reviewed in Ref. 13). A relatively minor direct association was detected between laminin-111 and type IV collagen that correlates with reduced recruitment of type IV collagen into the laminin cellular ECM in the absence of the nidogen-binding site. The immunohistochemical analyses of tissues of mice genetically modified to lack the nidogen-binding site in laminin γ1 or to lack expression of both nidogens have revealed only a limited decrease in the type IV collagen in those tissues examined (19, 21, 35) compared with that observed in this study. The mouse genetic data provide an argument for the existence of an additional mechanism by which type IV collagen can be recruited to laminin immobilized on cell surfaces, *i.e.* some of the nidogen-binding site mutant mice survive to but not beyond birth, whereas the type IV collagen knock-out mice do not survive beyond E11. One contributing mechanism may be a laminin-collagen interaction. Because the repertoire of laminins becomes more diverse as development proceeds, it is also possible that type IV collagen binds more avidly to laminins other than laminin-111. Furthermore, type IV collagen can be linked to laminin through the heparan sulfate proteoglycan, perlecan, a component known to bind to the two proteins (36).

In conclusion, the findings of this study provide a more comprehensive model of the role of laminin polymerization in basement membrane assembly, distinguishing contributions arising from the LN, LG, and nidogen-binding domain of laminin-111. The findings lead to predictions that could be tested in genetic models, among them that selective knock-out of laminin polymerization through a γ1- or β1-LN deletion should diminish basement membrane formation, especially in combination with loss of nidogen binding.

Acknowledgment—We thank Raj Patel (Robert Wood Johnson Medical School) for preparing cell samples for electron microscopy.

REFERENCES

1. Aumailley, M., Bruckner-Tuderman, L., Carter, W. G., Deutzmann, R., Edgar, D., Ekblom, P., Engel, J., Engvall, E., Hohenester, E., Jones, J. C., Kleinman, H. K., Marinkovich, M. P., Martin, G. R., Mayer, U., Meneguzzi, G., Miner, J. H., Miyazaki, K., Patarroyo, M., Paulsson, M., Quaranta, V., Sanes, J. R., Sasaki, T., Sekiguchi, K., Sorokin, L. M., Talts, J. F., Tryggvason, K., Uitto, J., Virtanen, I., von der Mark, K., Wewer, U. M., Yamada, Y., and Yurchenco, P. D. (2005) *Matrix Biol.* **24,** 326–332
2. Cheng, Y. S., Champliaud, M. F., Burgeson, R. E., Marinkovich, M. P., and Yurchenco, P. D. (1997) *J. Biol. Chem.* **272,** 31525–31532
3. Yurchenco, P. D., and Cheng, Y. S. (1993) *J. Biol. Chem.* **268,** 17286–17299
4. Yurchenco, P. D., Cheng, Y. S., and Colognato, H. (1992) *J. Cell Biol.* **117,** 1119–1133
5. Yurchenco, P. D., Tsilibary, E. C., Charonis, A. S., and Furthmayr, H. (1985) *J. Biol. Chem.* **260,** 7636–7644
6. Paulsson, M. (1988) *J. Biol. Chem.* **263,** 5425–5430
7. Odenthal, U., Haehn, S., Tunggal, P., Merkl, B., Schomburg, D., Frie, C., Paulsson, M., and Smyth, N. (2004) *J. Biol. Chem.* **279,** 44505–44512
8. Ruben, G. C., and Yurchenco, P. D. (1994) *Microsc. Res. Tech.* **28,** 13–28
9. Yurchenco, P. D., and Ruben, G. C. (1987) *J. Cell Biol.* **105,** 2559–2568
10. Fox, J. W., Mayer, U., Nischt, R., Aumailley, M., Reinhardt, D., Wiedemann, H., Mann, K., Timpl, R., Krieg, T., Engel, J., and Chu, M. L. (1991) *EMBO J.* **10,** 3137–3146
11. Pöschl, E., Mayer, U., Stetefeld, J., Baumgartner, R., Holak, T. A., Huber, R., and Timpl, R. (1996) *EMBO J.* **15,** 5154–5159
12. Ries, A., Gohring, W., Fox, J. W., Timpl, R., and Sasaki, T. (2001) *Eur. J. Biochem.* **268,** 5119–5128
13. Timpl, R., and Brown, J. C. (1996) *BioEssays* **18,** 123–132
14. Huang, C. C., Hall, D. H., Hedgecock, E. M., Kao, G., Karantza, V., Vogel, B. E., Hutter, H., Chisholm, A. D., Yurchenco, P. D., and Wadsworth, W. G. (2003) *Development* (*Camb.*) **130,** 3343–3358
15. Yurchenco, P. D., Amenta, P. S., and Patton, B. L. (2004) *Matrix Biol.* **22,** 521–538
16. Chen, Z. L., and Strickland, S. (2003) *J. Cell Biol.* **163,** 889–899
17. Smyth, N., Vatansever, H. S., Murray, P., Meyer, M., Frie, C., Paulsson, M., and Edgar, D. (1999) *J. Cell Biol.* **144,** 151–160
18. Miner, J. H., Li, C., Mudd, J. L., Go, G., and Sutherland, A. E. (2004) *Development* (*Camb.*) **131,** 2247–2256
19. Willem, M., Miosge, N., Halfter, W., Smyth, N., Jannetti, I., Burghart, E., Timpl, R., and Mayer, U. (2002) *Development* (*Camb.*) **129,** 2711–2722
20. Pöschl, E., Schlotzer-Schrehardt, U., Brachvogel, B., Saito, K., Ninomiya, Y., and Mayer, U. (2004) *Development* (*Camb.*) **131,** 1619–1628
21. Bose, K., Nischt, R., Page, A., Bader, B. L., Paulsson, M., and Smyth, N. (2006) *J. Biol. Chem.* **281,** 11573–11581
22. Sunada, Y., Bernier, S. M., Utani, A., Yamada, Y., and Campbell, K. P. (1995) *Hum. Mol. Genet.* **4,** 1055–1061
23. Colognato, H., and Yurchenco, P. D. (1999) *Curr. Biol.* **9,** 1327–1330
24. Li, S., Harrison, D., Carbonetto, S., Fässler, R., Smyth, N., Edgar, D., and Yurchenco, P. D. (2002) *J. Cell Biol.* **157,** 1279–1290
25. Li, S., Liquari, P., McKee, K. K., Harrison, D., Patel, R., Lee, S., and Yurchenco, P. D. (2005) *J. Cell Biol.* **169,** 179–189
26. Moll, J., Barzaghi, P., Lin, S., Bezakova, G., Lochmuller, H., Engvall, E., Müller, U., and Ruegg, M. A. (2001) *Nature* **413,** 302–307
27. Yurchenco, P. D., Quan, Y., Colognato, H., Mathus, T., Harrison, D., Yamada, Y., and O'Rear, J. J. (1997) *Proc. Natl. Acad. Sci. U. S. A.* **94,** 10189–10194
28. Smirnov, S. P., McDearmon, E. L., Li, S., Ervasti, J. M., Tryggvason, K., and Yurchenco, P. D. (2002) *J. Biol. Chem.* **277,** 18928–18937
29. Colognato-Pyke, H., O'Rear, J. J., Yamada, Y., Carbonetto, S., Cheng, Y. S., and Yurchenco, P. D. (1995) *J. Biol. Chem.* **270,** 9398–9406
30. Yurchenco, P. D., and Furthmayr, H. (1984) *Biochemistry* **23,** 1839–1850
31. Tsiper, M. V., and Yurchenco, P. D. (2002) *J. Cell Sci.* **115,** 1005–1015
32. Pöschl, E., Fox, J. W., Block, D., Mayer, U., and Timpl, R. (1994) *EMBO J.* **13,** 3741–3747
33. Harrison, D., Hussain, S. A., Combs, A. C., Ervasti, J. M., Yurchenco, P. D., and Hohenester, E. (2007) *J. Biol. Chem.* **282,** 11573–11581
34. Kalb, E., and Engel, J. (1991) *J. Biol. Chem.* **266,** 19047–19052
35. Bader, B. L., Smyth, N., Nedbal, S., Miosge, N., Baranowsky, A., Mokkapati, S., Murshed, M., and Nischt, R. (2005) *Mol. Cell. Biol.* **25,** 6846–6856
36. Fujiwara, S., Wiedemann, H., Timpl, R., Lustig, A., and Engel, J. (1984) *Eur. J. Biochem.* **143,** 145–157